Antiproliferative, Anti-Inflammatory and Anti-Microbial Activities of Synthesized Benzo[*f*]benzo[4,5]imidazo[1,2-*d*][1,4]oxazepine and Benzo[*f*]benzo[4,5]oxazolo[3,2-*d*][1,4]oxazepine Derivatives

Khalid M. Abu Khadra, [a] *Huda A. AL-Saadi,*[b] *Areej M. Assaf,*[c] *Firas F. Awwadi*[d] *and Shehadeh Mizyed* *,[b]

aDepartment of Biological Sciences, Yarmouk University, Irbid 21163, Jordan

bChemistry Department, Yarmouk University, Irbid 21163, Jordan

cSchool of Pharmacy, The University of Jordan, Amman 11942, Jordan

dChemistry Department, Faculty of Science, The University of Jordan, Amman 11942, Jordan

Synthesized benzoxazepine derivatives have been characterized and evaluated using ^{1}H, ^{13}C nuclear magnetic resonance (NMR), DEPT 135 (distortionless enhancement by polarization transfer), and high resolution mass spectrometry (HRMS) to confirm the leading benzoxazepine chemical structures. X-ray crystal structure of compounds **10** and **13** (10,11-dimethyl-6,7-dihydrobenzo[*f*]benzo[4,5]imidazo[1,2-*d*][1,4]oxazepine and 8,9-dihydrobenzo [4,5]imidazo[1,2-*d*]naphtho[1,2-*f*][1,4]oxazepine) were obtained after successful diffraction of the compound crystals. The anti-microbial, anti-cancer and anti-inflammatory activities of the synthesized benzoxazepine derivatives were evaluated. The effect of benzoxazepine derivatives on cancer cell proliferation and microbial growth was studied. Our results revealed limited antimicrobial activity to the synthesized benzoxazepine derivatives with significant activities against certain bacterial pathogens for two compounds. The synthesized benzoxazepine derivatives displayed cytotoxicity against selected solid tumor cell lines with varying effects on the release of human interleukin-6 (IL-6) and tumor necrosis factor-α (TNF-α) pro-inflammatory cytokines depending on the cancer cell type used. The results of the study suggest that the synthesized benzoxazepine derivatives show anti-cancer and anti-inflammatory agents, though with dependence on the type of cancer cell line.

Keywords: benzoxazepine derivatives, heterocyclic compounds, X-ray structures, anti-cancer, anti-inflammatory and anti-microbial activities

Introduction

Benzoxazepine derivatives have a wide range of biological and pharmaceutical activities including antipsychotic,[1] anticonvulsant,[2] neuroleptic,[3] and central nervous system activity inhibitors.[4] Benzoxazepine derivatives could be potent candidates as chemotherapeutic agents for the treatment of different diseases including bacterial infections and cancer.

Cancer was the second-leading cause of worldwide death in 2020.[5] Over the past years, there is an imperative requirement to synthesize efficient and safe chemotherapeutic agents that can fight cancer by inhibiting cancer cell proliferation, invasion, and metastasis.[6] Drug designing has a high dependence on synthetic chemistry. In this regard, the design and development of such chemotherapeutic agents derived from benzoxazepine that have previously reported biological activities are still significant in synthetic chemistry.[7]

Several methods for the synthesis of benzoxazepines have been reported.[8-11] Some benzoxazepines derivatives were prepared as transit molecules during the synthesis of substituted benzoxazepines by Mannich reaction.[12] The synthesis of 2,3,4,5-tetrahydro-1,4-benzoxazepines involves the reduction of the carbonyl group of 5-oxo-2,3,4,5-tetra-hydro-1,4-benzoxazepine or 3-oxo-2,3,4,5-tetrahydro-1,4-benzoxazepine.[13-16] Levan *et al.*[17] reported the synthesis of unsubstituted 1,2,3,5,6,11*b*-hexahydroimidazo [1,2-*d*][1,4]benzoxazepine. As part of our ongoing
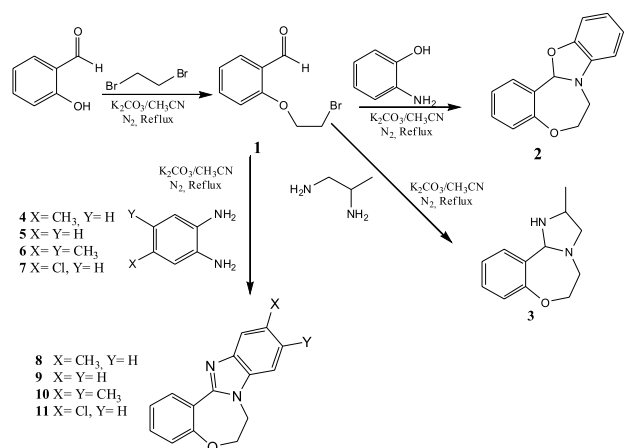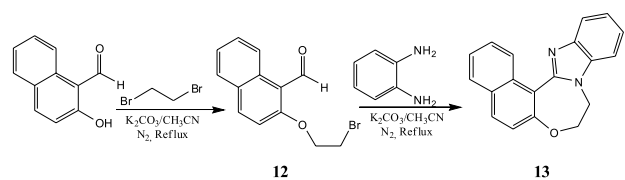
research for the synthesis of Schiff base crown ethers, we accidentally obtained benzoxazepine compounds as unexpected products in a simple one-step reaction. The method was further verified with different starting materials, and X-ray crystal structural data supported the successful synthesis of two of these compounds.[18] These compounds are considered unique for having a tricyclic system with 5-, 6- and 7-membered rings including oxygen and nitrogen hetero atoms. Later, another new series of [1,4]benzoxazepine derivatives have been synthesized by incorporating 1,3-oxazolidine, 1,3-oxazinane or hexahydropyrimidine rings onto a [1,4]benzoxazepine ring.[19] The method is simply a condensation of 2-aminoethanol, 3-amino-1-propanol or 1,3-diamino propane with 2-(2-bromoethoxy) benzaldehydes in acetonitrile in the presence of anhydrous potassium carbonate as a base at reflux temperature.[19] A proposed mechanism for the formation of the products was also reported. The above procedure succeeded when aliphatic and aromatic diamines were used, with some 2- or 3-amino alcohols. However, it failed to give the desired product with 2-aminophenol. This motivated us to follow this approach on other diamines, and aldehydes and re-examine this general procedure with aminophenol.

In this paper, we report the synthesis of a new series of benzoxazepine derivatives (**2**, **3** and **8-11**) including **2** (which was prepared from 2-aminophenol) shown in Scheme 1 and re-synthesis of **13** shown in Scheme 2 which was previously reported.[19] The X-ray structures of compounds **10** and **13**,

and the biological, anti-proliferative and anti-cancer potential of compounds (**2**, **3**, **8-11** and **13**) are reported.

Experimental

Materials and equipment

General

All reagents were of analytical grade and used without further purification, only CH₃CN was distilled before use and the diamines were purified by either sublimation or recrystallization. Silica gel 60 for column chromatography was obtained from Fluka (Darmstadt, Germany). 1,2-Dibromoethane was obtained from Sigma-Aldrich (Schnelldorf, Germany); salicylaldehyde and naphthaldehyde from Lancaster Synthesis (Lancaster, UK); diamines and *o*-aminophenol were purchased from Acros-Organics (Geel, Belgium); anhydrous potassium carbonate from Sure Chem (Shijiazhuang, China), and acetonitrile was obtained from TEDIA (Fairfield, OH, USA). Melting points are uncorrected and obtained on electrothermal melting point apparatus from TEquipment (NJ, USA). The ¹H and ¹³C nuclear magnetic resonance (NMR) spectra were recorded on 400 and 100 MHz, respectively, using Bruker Avance (III) 400 MHz (Uster, Swizzerland). Chemical shifts were recorded using (CDCl₃, 1% tetramethylsilane (TMS)) or C₂D₆SO (dimethyl sulfoxide (DMSO-d_6)) as solvents. High resolution mass spectrometry (HRMS) measured as (positive or negative ion mode) were determined using the electrospray ion trap (ESI) technique by collision-include dissociation on a Bruker APEX-IV (7 Tesla) instrument, Germany, and X-ray data were collected on a Xcalibur, Eos diffractometer from Bruker, Germany. Chromatographic separations were performed on silica gel columns (60-120 mesh, CDH) using (ethylacetate:hexane) as a solvent system. All reactions were carried out under dry nitrogen. Compounds **1** and **12** are synthesized according to the published procedures.[20] The structures were confirmed using ¹H and ¹³C NMR. The data is consistent with the published data.

General procedure for the synthesis of benzoxazepines

In a 250 mL three-necked flask with a magnetic stirrer bar and a reflux condenser under a nitrogen atmosphere, a 0.49 g (3.6 mmol) of anhydrous K₂CO₃ was suspended in 100 mL of anhydrous CH₃CN. To this solution, with stirring at reflux temperature, a solution of aldehyde (1.8 mmol) in 50 mL dry CH₃CN and a solution of diamine or aminophenol (1.8 mmol) in 50 mL of dry CH₃CN were dropwise added simultaneously over a period of 12 h. The reaction mixture was further refluxed by stirring

Scheme 1. Synthesized benzoxazepine derivatives **2**, **3** and **8-11**.

Scheme 2. Synthesis of compound **13**.

overnight. The reaction mixture was filtered, and the solvent was evaporated. The crude product was purified by chromatographic separation.

Synthesis of 6,7-dihydro-13a*H*-benzo[*f*]benzo[4,5]oxazolo[3,2-*d*][1,4]oxazepine (2)

The crude product was purified by column chromatography on silica gel using hexane:ethyl acetate (8.5:1.5) in a yield of 0.14 g (33%). mp:163-165 ºC; ^{1}H NMR (400 MHz, CDCl$_3$) δ 4.02 (2H, t, *J* 5.1Hz, C$\underline{H}_2$–N), 4.61 (2H, t, *J* 5.1 Hz, C$\underline{H}_2$), 7.04 (1H, t, *J* 7.6 Hz, Ar$\underline{H}$), 7.13 (2H, t, *J* 8.0 Hz, Ar$\underline{H}$), 7.21-7.28 (4H, m, Ar$\underline{H}$), 7.54 (1H, t, *J* 7.6 Hz, Ar$\underline{H}$), 7.93 (1H, d, *J* 7.8 Hz, Ar$\underline{H}$); ^{13}C NMR (100 MHz, CDCl$_3$) δ 51.1, 73.8, 76.7, 120.4, 121.6, 123.9, 124.5, 126.2, 128.8, 131.7, 132.1, 133.9, 151.3, 154.1, 169.6; DEPT 135: showed two negative signals at 51.1 and 73.8 ppm; HRMS (ESI) *m/z*, calculd. for C$_{15}$H$_{13}$KNO$_2$ [M + K]$^+$: 278.05834, found 278.05837 a.m.u.

Synthesis of 3-methyl-2,3,5,6-tetrahydrobenzo[*f*]imidazo[1, 2-*d*][1,4]oxazepine (3)

The crude product was purified by plate chromatography on silica gel using ethyl acetate:methanol (9:1) as a brown semi-solid in a yield of (0.12g, 33%). ^{1}H NMR (400 MHz, CDCl$_3$) δ 1.10 (3H, d, *J* 6.0 Hz, C$\underline{H}_3$), 2.11(1H, bs, N$\underline{H}$), 2.65-2.67 (1H, m, N-C$\underline{H}$-CH$_2$-N), 2.72-2.79 (2H, m, N-C(CH$_3$)H-C$\underline{H}_2$-N), 3.16 (1H, d, *J* 12.0 Hz, N-C$\underline{H}_2$-CH$_2$-O), 3.23-3.28 (1H, m, N-C$\underline{H}_2$-CH$_2$-O), 3.76 (1H, t, *J* 11.6 Hz, N-CH$_2$-C$\underline{H}_2$-O), 4.32 (1H, d, *J* 12.0 Hz, N-CH$_2$-C$\underline{H}_2$-O), 4.51 (1H, s, N-C$\underline{H}$-NH), 6.94 (1H, d, *J* 7.8 Hz, Ar$\underline{H}$), 7.01 (1H, t, *J* 7.6 Hz, Ar$\underline{H}$), 7.13 (1H, t, *J* 7.8 Hz, Ar$\underline{H}$), 7.49 (1H, d, *J* 7.8 Hz, Ar$\underline{H}$); ^{13}C NMR (100 MHz, CDCl$_3$) δ 18.2, 51.7, 54.6, 62.1, 72.5, 79.9, 121.1, 123.8, 126.1, 128.7, 133.9, 158.7;DEPT 135: showed three negative signals at 51.67, 54.56 and 72.57 ppm for the two methylene groups in the seven membered ring and the third is for the methylene group in the five membered ring. It also showed three positive signals in the aliphatic region at 18.16, 62.09 and 79.96 for the methyl group and two CH groups in the five membered ring; HRMS (ESI) *m/z*, calcd. for C$_{12}$H$_{16}$N$_2$O [M + H]$^+$: 205.13409, found 205.132340 a.m.u.

Synthesis of 11-methyl-6,7-dihydrobenzo[*f*]benzo[4,5]imidazo[1,2-*d*][1,4]oxazepane (8)

The crude product was purified by column chromatography on silica gel using hexane:ethyl acetate (9.5:0.5) in a yield of (0.24, 53%). mp 113-116 ºC; ^{1}H NMR (400 MHz, CDCl$_3$) δ 2.50 (3H, s, C$\underline{H}_3$), 4.49 (2H, t, *J* 4.4 Hz, C$\underline{H}_2$), 4.59 (2H, t, *J* 4.4 Hz, C$\underline{H}_2$), 7.07-7.23 (4H, m, Ar$\underline{H}$), 7.35 (1H, t, *J* 8.4 Hz, Ar$\underline{H}$), 7.61 (1H, s, Ar$\underline{H}$),

8.74 (1H, d, *J* 8.0 Hz, Ar$\underline{H}$); ^{13}C NMR (100 MHz, CDCl$_3$) δ 21.7, 47.1, 68.9, 108.6, 118.8, 119.5, 120.7, 123.1, 124.3, 131.2, 131.7, 131.1, 131.7, 132.5, 134.5 143.0, 150.0, 157.0; DEPT 135: two negative signals at 47.1 and 68.9 ppm for the two methylene groups in the seven-membered ring, and eight positive signals at 21.7 for the methyl group and 108.6, 119.5, 120.7, 123.1, 124.3, 131.2 and 131.7 for the aromatic CH groups; HRMS (ESI) *m/z*, calcd. for C$_{16}$H$_{14}$N$_2$O [M + H]$^+$: 251.11061, found 251.11872 a.m.u.

Synthesis of 6,7-dihydrobenzo[*f*]benzo[4,5]imidazo[1,2-*d*][1,4]oxazepine (9)

The product was obtained after purification by column chromatography on silica gel using hexane:ethyl acetate as (8.5:1.5) to give a pale-yellow solid in a yield of (0.23 g, 54%); mp 114-117 ºC; ^{1}H NMR (400 MHz, CDCl$_3$) δ 4.47 (2H, t, *J* 3.6 Hz, C$\underline{H}_2$), 4.54 (2H, t, *J* 3.6 Hz, C$\underline{H}_2$), 7.03 (1H, d, *J* 8.0 Hz, Ar$\underline{H}$), 7.13 (1H, t, *J* 7.8 Hz, Ar$\underline{H}$), 7.23-7.32 (4H, m, Ar$\underline{H}$), 7.77 (1H, d, *J* 4.0 Hz, Ar$\underline{H}$), 8.70 (1H, d, *J* 8.0 Hz, Ar$\underline{H}$); ^{13}C NMR (100 MHz, CDCl$_3$) δ 47.1, 68.9, 109.1, 118.6, 119.7, 120.7, 122.8, 122.9, 123.1, 131.4, 131.7, 136.3, 142.7, 150.2, 157.1; DEPT 135: negative at 47.1 and 68.9 ppm; positive at 109.1, 119.7, 120.7, 122.8, 122.9, 123.1, 131.4, 131.4 eight C--H; HRMS (ESI) *m/z*, calcd. for C$_{15}$H$_{12}$N$_2$O [M + H]$^+$: 237.09496, found 237.10291 a.m.u.

Synthesis of 10,11-dimethyl-6,7-dihydrobenzo[*f*]benzo[4,5]imidazo[1,2-*d*][1,4]oxazepine (10)

The light brown product (0.28 g, 59%) yield; mp 168-170 ºC was isolated and characterized; ^{1}H NMR (400 MHz, CDCl$_3$) δ 2.32 (3H, s, C$\underline{H}_3$), 2.34 (3H, s, C$\underline{H}_3$), 4.43 (2H, t, *J* 4.2 Hz, C$\underline{H}_2$), 4.52 (2H, t, *J* 4.2 Hz, C$\underline{H}_2$), 7.01 (1H, d, *J* 8.0 Hz, Ar$\underline{H}$), 7.06 (1H, s, Ar$\underline{H}$), 7.13 (1H, t, *J* 7.6 Hz, Ar$\underline{H}$), 7.29 (1H, t, *J* 7.6 Hz, Ar$\underline{H}$), 7.56 (1H, s, Ar$\underline{H}$), 8.69 (1H, d, *J* 8.0 Hz, Ar$\underline{H}$); ^{13}C NMR (100 MHz, CDCl$_3$) δ 20.4, 20.7, 47.3, 68.8, 109.5, 119.3, 120.7, 123.3, 131.4, 131.6, 132.4, 132.6, 134.5, 148.8, 157.0; DEPT135: positive signals at 20.4, 20.7 (for the methyl groups), 109.5, 119.3, 120.7, 123.3, 131.4, 131.6 ppm (for the six aromatic C–H bonds) and two negative signals at 47.3 and 68.8 for the two methylene groups in the seven membered ring; HRMS (ESI) *m/z*, calcd. for C$_{17}$H$_{16}$N$_2$O [M + H]$^+$ 265.13409, found 265.13459 a.m.u.

Synthesis of 11-chloro-6,7-dihydrobenzo[*f*]benzo[4,5]imidazo[1,2-*d*][1,4]oxazepine (11)

The crude product was purified by column chromatography on silica gel using hexane:ethyl acetate (9.75:0.25) to give a white solid in a yield of (0.38 g, 78%); mp 96-98 ºC; ^{1}H NMR (400 MHz, CDCl$_3$) δ 4.42 (2H, t,

J 4.2 Hz, C$\underline{H}_2$), 4.54 (2H, t, *J* 4.2 Hz, C$\underline{H}_2$), 7.03 (1H, d, *J* 8.2 Hz, Ar$\underline{H}$), 7.13 (1H, t, *J* 8.2 Hz, Ar$\underline{H}$), 7.28-7.34 (3H, m, Ar$\underline{H}$), 7.66 (1H, d, *J* 8.1 Hz, Ar$\underline{H}$, 8.66 (1H, d, *J* 8.1 Hz, Ar); ^{13}C NMR (100 MHz, CDCl$_3$) *δ* 47.3, 68.8, 109.3, 109.9, 118.2, 119.4, 120.5, 120.8, 123.2, 123.6, 128.5, 131.7, 131.8, 135.0, 143.5, 157.2; DEPT 135 showed two negative signals at 47.3 and 68.8 ppm; HRMS (ESI) *m/z,* calcd. for C$_{15}$H$_{11}$ClN$_2$O [M + H]$^+$: 271.06381, found 271.06426 a.m.u. The [M + H + 2]$^+$ signal at 273.06103 a.m.u. with 1/3 height of the original signal indicates a Cl containing compound.

Synthesis of 8,9-dihydrobenzo [4,5]imidazo[1,2-*d*] naphtho[1,2-*f*][1,4]oxazepine (13)

The product was prepared as previously reported.[19]

Antimicrobial susceptibility testing

The sensitivity and susceptibility of bacterial pathogens to compounds **2**, **3**, **8-11** and **13** were used to assess their expected potential biological activity. Disk diffusion antibiotic sensitivity testing was used to perform antimicrobial susceptibility testing for the compounds compared to tetracyclene as a control. The test utilizes soaked sterilized filter paper (discs 6 mm in diameter) with the test compounds that had been dissolved in DMSO. Four common pathogens were used in the antimicrobial susceptibility testing of these chemically synthesized compounds. The common pathogens are *Pseudomonas aeruginosa*, *Escherichia coli*, *Staphylococcus aureus* and *Bacillus cereus*. Furthermore, the antifungal susceptibility testing for compounds **2**, **3**, **8**-**11** and **13** was carried out for *Candida albicans*. The tested organism was subcultured by applying an inoculum of approximately (1-2 × 10^8 colony forming units (CFU) mL^{-1}) to the surface of a large (150 mm diameter) fresh Muller Hinton agar plate. The subculture was performed as follows, starting at the top of the plate and covering the entire plate by streaking back and forth from edge to edge. The sterilized filter paper was soaked with two different concentrations (10 and 20 μg) of each compound and was dried before being placed on the Petri dishes (120 mm in diameter) that were inoculated with the tested organisms of the previously listed strain of bacteria. The plates were incubated at 37 °C. The antibacterial activity of the synthesized compounds was determined according to the zone of inhibition by measuring the diameter of the zone of inhibition in mm. The organism that is susceptible to the tested compounds shows an area of clearing surrounding the corresponding impregnated filter paper called the zone of inhibition. The zone of inhibition surrounding the corresponding impregnated disc indicates that bacteria are not capable of growing because of the bactericidal or bacteriostatic action of the tested compound. The diameter of the zone of inhibition correlates with the inhibitory concentration of the corresponding compound for that organism.

Cell lines and cultivation conditions

Human cervical adenocarcinoma (HeLa), adenocarcinoma human alveolar basal epithelial cells (A549), human breast cancer (MCF-7), Caucasian colon adenocarcinoma Caco-2, and human fibroblast cell lines (F2) were grown in Dulbecco's modified Eagle's minimal essential medium (DMEM), supplemented with 25 mM glucose, 10% inactivated fetal bovine serum (Flow, McLean, VA, USA), and 1% penicillin/streptomycin, and maintained at 37 °C in a humidified incubator with 5% CO$_2$. The cells with 30-40 passages were used for further investigations.

Cell lines and tested compounds

The synthesized compounds **9**, **10**, **11**, and **13**, were dissolved in DMSO to the final concentration of 20 μg L^{-1}. The DMSO concentration was less than 1.0% in all experiments and controls. The compounds were evaluated for their anti-proliferative activity against HeLa, A549, Caco-II, MCF-7 cancer cell lines compared to the normal human periodontal ligament (HPDL) and to cells alone as a negative control. Cisplatin, one of the most potent and widely used drugs for the treatment of various solid cancers, was used as a control.

Cytotoxic activity (MTT assay) and IC$_{50}$ values of the synthesized compounds

Exponentially growing cells have been seeded at 3 × 10^4 cells *per* well (100 μL *per* well) in 96 well microplates (Greiner, Germany). After 24 h, cells were confluent, and media was changed and cells were incubated with various concentrations of the tested compounds (200-1 μg mL^{-1}) for 24 h. *In vitro* anti-proliferative activity was measured by the cell growth inhibition assay using 3-(4,5-dimethyl-thiazol-2-yl)-2,5-di-phenyltetrazolium bromide (MTT) assay according to the instructions of the manufacturer (Promega Corporation, Madison, USA). Briefly, the assay measured the formation of blue formazan product as a result of the reduction of MTT by mitochondrial dehydrogenase, which indicates the normal function of mitochondria and cell viability. The amount of formazan was quantified using a microplate reader (Thermo

Fisher Scientific, Waltham, MA, USA) and compared to the optical density obtained for the control (untreated) at 570 nm. The half-maximal inhibitory concentration (IC$_{50}$) values were calculated according to the equation for Boltzmann sigmoidal concentration response curve using the nonlinear regression models (GraphPad, Prism, version 7, San Diego, CA, USA).[21] The antiproliferative activities of the investigated compounds were expressed in IC$_{50}$ values (the concentration needed to inhibit 50% of cell growth compared to untreated cells). IC$_{50}$ values were reported as the average of three replicates.

Effects of the synthesized compounds on the production of human pro-inflammatory cytokines interleukin-6 (IL-6) and tumor necrosis factor-α (TNF-α)

To determine the effect of the tested compounds *in vitro*, 1×10^6 cells mL^{-1} of each cancer cell line were seeded in a 24-well plate and either left for 60 min before the treatment with the compounds and the control drug, cisplatin. Cells were then treated with one of the tested compounds at 1, 5, 10, 25, and 50 μg mL^{-1} concentrations separately in a growth medium or left without treatment (control). Cultures were incubated in a humidified atmosphere of 37 °C and 5% CO$_2$ overnight. Supernatants obtained from controls and treated cells were harvested for analysis by an enzyme-linked immunosorbent assay (ELISA). Non-treated cells were used as negative controls. The concentrations of IL-6 and TNF-α cytokines (in 100 μL of cancer cell lines' supernatants) were determined by ELISA Ready-SET-Go e-Bioscience kit according to the manufacturer's protocol (Bioscience, San Diego, USA). All incubation steps were performed at room temperature. The optical density at 450 nm, corrected by the reference wavelength 570 nm, was measured with a microplate reader (Biotek, Winooski, VT, USA). All cytokine assays were calibrated against the World Health Organization's international standards by the kit's manufacturer. The lower limit of detection for the individual assays for human IL-6 was 2 pg mL^{-1} and 4 pg mL^{-1} for TNF-α.

Crystal structure determination

Suitable crystals of compounds **10** and **13** were selected and diffraction data were collected on a Xcalibur, Eos diffractometer.[22] Data were acquired and processed to give SHELX-format-*hkl* files using CrysAlisPro software. Cell parameters were determined and refined using CrysAlisPro.[22] A multiscan absorption collection was applied. The crystal was kept at 293(2) K during data collection. Using Olex2,[23] the structure was solved with the SHELXT[24] structure solution program using intrinsic

phasing and refined with the SHELXL[25] refinement package using least squares minimization. All atoms are refined anistropically except hydrogen atoms that are located in the calculated positions. Data collection and refinement parameters are listed in Table 1.

Results and Discussion

All new compounds were characterized by ^{1}H and ^{13}C, ^{13}C DEPT 135 NMR spectroscopy, and HRMS. The mass spectra of our compounds displayed the correct molecular ion peaks for which the HRMS data are in good agreement with the calculated values. The NMR data are consistent with the suggested structures. ^{1}H NMR spectra of compounds **2**, **3**, **8-11**, and **13** have identical two-triplet patterns in the chemical shift range of δ ca. 4.4-4.6 ppm, assigned for the C$\underline{H}_2$−C$\underline{H}_2$ groups within the seven-membered ring. The signals of the proton and the carbon atoms of CHNN segment which usually show up as sharp singlet signals around 4.6 ppm in the ^{1}H NMR and 79 ppm in the ^{13}C NMR spectra are considered strong evidence for the formation of the five membered ring. These signals are only shown in compound **3**. However, they did not show up in the products where aromatic diamines or aminophenol are used; providing evidence that a N−C=N group is formed. The HRMS data confirms this finding. Further evidence for the formation of the N−C=N group comes from the X-ray data of compounds **10** and **13** which reveal that the C=N bond distances are shorter than other single bonds and confirm the double bonds character. The formation of this double bond is driven by the formation of an aromatic ring, is not formed when 2,3-diamino propane was used to form compound **3**. The NMR spectral data reveals the disappearance of the aldehyde carbonyl signal at about 200 ppm in the ^{13}C NMR spectrum and at about 9 ppm for the aldehyde proton in the ^{1}H NMR spectrum. DEPT results give the appropriate CH, CH$_2$, and CH$_3$ signals.

The ^{1}H NMR spectrum showed clearly the presence of the methylene groups at 4.44 and 4.54 ppm, and the ^{13}C NMR spectrum also showed the presence of methylene groups at 47.3 and 68.8 ppm. The formation of compounds **3**, **8** and **11** is expected to give two regioisomers; we are unable to determine which of the isomers is isolated, but this explains the duplication of some peaks in the ^{13}C NMR spectrum. Recently, Srinivasulu *et al.*[11] reported the formation of similar regioisomers.

A plausible reaction mechanism was proposed by Ashram *et al.*[19] for the formation of these tricyclic scaffolds [1,4] benzoxazepines. This mechanism does not show the formation of the imidazole aromatic ring formed in our compounds. However, Srinivasulu *et al.*[11] reported

Table 1. Data collection and refinement parameters of compounds **10** and **13**

Compound	10	13
Empirical formula	$C_{17}H_{16}N_2O$	$C_{19}H_{14}N_2O$
Formula weight / (g mol^{-1})	264.32	286.32
Temperature / K	293(2)	293(2)
Crystal system	monoclinic	monoclinic
Crystal habit	fragment	fragment
Crystal color	yellow	yellow
Crystal size / mm^3	$0.2 \times 0.1 \times 0.05$	$0.2 \times 0.2 \times 0.2$
Space group	P2$_1$/c	C2/c
a / Å	11.4913(9)	23.4986(13)
b / Å	6.8496(7)	8.6134(2)
c / Å	17.5882(19)	18.1262(10)
β / degree	100.353(9)	128.727(9)
Volume / Å^3	1361.8(2)	2862.2(4)
CCDC No.	2233685	2233684
Z	4	8
ρ_{calc} / (g cm^3)	1.289	1.329
μ / mm^1	0.081	0.084
F(000)	560.0	1200.0
Absorption correction type	multi-scan	multi-scan
Transmission factors	0.78693-1.00000	0.76208-1.0000
2Θ range for data collection / degree	6.398 to 57.976	5.762 to 58.206
Radiation	Mo Kα (λ = 0.71073)	Mo Kα (λ = 0.71073)
Index ranges	$-14 \le h \le 15, -6 \le k \le 8, -20 \le l \le 21$	$-29 \le h \le 29, -11 \le k \le 6, -24 \le l \le 21$
Reflections collected	6577	6548
Independent reflections	3110 [R_{int} = 0.0290, R_{sigma} = 0.0656]	3281 [R_{int} = 0.0163, R_{sigma} = 0.0290]
Data/restraints/parameters	3110/0/183	3281/0/199
Goodness-of-fit on F^2	1.012	1.027
Final R indexes [I > = 2σ (I)]	R_1^a = 0.0631, wR_2^b = 0.1362	R_1^a = 0.0482, wR_2^b = 0.1181
Final R indexes [all data]	R_1^a = 0.1558, wR_2^b = 0.1726	R_1^a = 0.0679, wR_2^b = 0.1305
Largest diff. peak/hole / (e Å^{-3})	0.25/-0.14	0.51/−0.19

Cell dimensions: a, b, and c; and β (degree); Z: number of formula units in the unit cells; ρ_{calc}: density; μ: radiation. $^aR_1 = \Sigma||F_o| - |F_c||/\Sigma|F_o|$, $^bwR_2 = \{\Sigma\ w(F_o^2 - F_c^2)^2/\Sigma w(F_o^2)^2\}^{1/2}$.

a one-pot synthesis of imidazole-fused benzoxazepines. Furthermore, Fujioka *et al.*[26] reported the formation of an imidazole system from the reaction of different aldehydes with several diamines at room temperature. Presumably, those cases can be applied to our system and explain the formation of the imidazole ring.

The reaction of compound **1** with *o*-aminophenol produced (**2**), the isolated products molecular ion peak contains 39 a.m.u more than expected due to K$^+$ ion that comes from K$_2$CO$_3$. The X-ray crystal structures of compounds **10** and **13** confirmed their proposed structures. The thermal ellipsoid structure σ of compounds **10** and **13** are shown in Figure 1 and selected bond distances and angles are listed in Table 2. Compound **10** is nearly planar (with the exception of the oxazepine ring), but

the deviation from planarity is more pronounced in compound **13** as indicated by the N1−C9−C2−C1 torsion angle in compound **10** which equals 7.9(4)°, whereas the corresponding torsion angle (N1−C13−C2−C1) in compound **13** is 43.8(2)° (Figures 1 and 2).

The conformation of the oxazepine rings is significantly different in both structures (Figures 1 and 2); the oxazepine ring is closer to the planarity in compound **10** than in **13**. The average deviation from the mean plane of oxazepine ring is 0.237 and 0.367 Å in compounds **10** and **13**, respectively. The larger size of the naphthyl group in compound **13** compared to the size of the phenyl group in compound **10** results in this difference. The bond distances (N2−C9 in compound **10** and N2−C13 in compound **13**) are 1.32 Å which is shorter than other N2−C bond distances
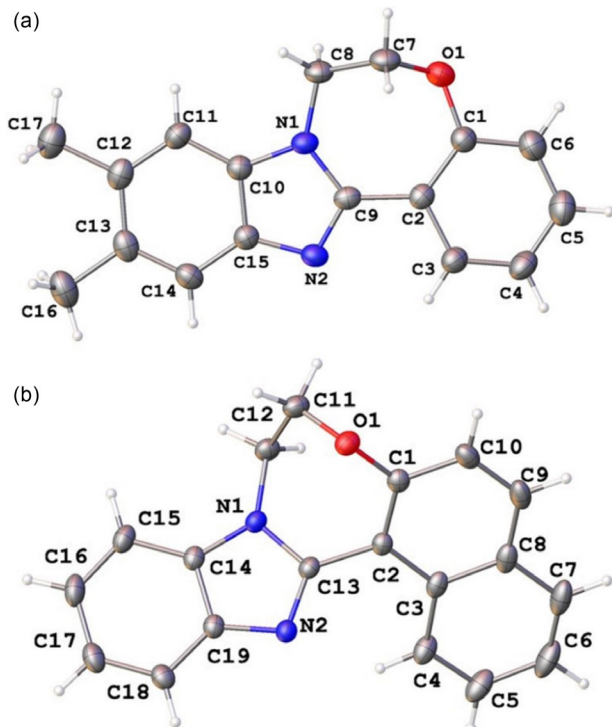
(a)

(b)

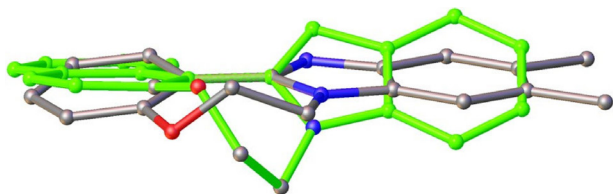**Figure 1.** Thermal ellipsoid structure of compounds **10** (a) and **13** (b).

Figure 2. Overlaid structure of compounds **10** and **13**. Compound **13** is shown in green.

for both compounds which reveals the C=N double bond characters of the N2=C9 and N2=C13 bonds.

Antimicrobial susceptibility effect

Antimicrobial susceptibilities of the synthesized compounds **2**, **3**, **8**, **9**, **10**, **11**, and **13** were conducted. Each compound was used in two different concentrations to test the potency and the effective concentration. Compounds **2**, **3**, **8**, **9**, **10** and **13** do not show any area of clearing surrounding the impregnated filter paper to any tested bacterial or fungal species. However, compound **11** and/or its regioisomer show a limited zone of inhibition surrounding the impregnated filter paper for Gram-positive and Gram-negative bacteria compared with that of tetracycline. The zone of inhibition around the impregnated disc with compound **11** and/or its regioisomer was less than 5 mm for *Pseudomonas aeruginosa* and *E. coli*. Compound **11** and/or its regioisomer showed limited but not significant zone of inhibition against *Candida* spp. Our

Table 2. Selected bond distances and angles of compounds **10** and **13**

Compound **10**		Compound **13**	
Bond distance / Å			
N1–C9	1.389(3)	N1–C13	1.3730(18)
N2–C9	1.320(3)	N2–C13	1.3194(19)
N1–C10	1.389(3	N1–C14	1.377(2)
N2–C15	1.397(3)	N2–C19	1.389(2)
O1–C1	1.368(3)	O1–C1	1.3858(19)
O1–C7	1.426(3)	O1–C11	1.429(2)
C2–C9	1.475(3)	C2–C13	1.468(2)
Angle / degree			
C9–N1–C8	130.9(2)	C13–N1–C12	123.66(13)
N1–C8–C7	112.8(2)	N1–C12–C11	111.24(13)
C8–C7–O1	112.0(2)	C12–C11–O1	112.97(14)
O1–C1–C2	124.1(2)	O1–C1–C2	120.34(14)
C1–O1–C7–C8	87.9(3)	C1–O1–C11–C12	44.2(2)
O1–C7–C8–N1	71.0(3)	O1–C11–C12–N1	40.7(2)
C7–C8–N1–C9	19.7(4)	C11–C12–N1–C13	69.28(19)
C8–N1–C9–C2	5.9(4)	C12–N1–C13–C2	3.2(2)
N1–C9–C2–C1	7.9(4)	N1–C13–C2–C1	43.84(19)
C9–C2–C1–O1	7.1(4)	C13–C2–C1–O1	4.6(2)
C2–C1–O1–C7	39.5(4)	C2–C1–O1–C11	75.53(18)

results indicate clearly that only compounds **11** and/or its regioisomer differ significantly from the other compounds in their activity against the tested microorganisms. These differences may be attributed to the chemical structure of compound **11** and/or its regioisomer. The existence of a chlorine atom in the chemical structure of compound **11** seems to be directly related to the antibacterial activity against certain pathogens whereas the chlorine atom in compound **11** as a halogen contributes directly to bacteriostatic action against microbes.[7]

Antiproliferative effect

The synthesized compounds **9**, **10**, **11**, and **13** were evaluated for their anti-proliferative and anti-inflammatory responses using various concentrations of each synthesized compound (Table 3). Screening the cytotoxic activity and IC_{50} values of the selected synthesized compounds and the control drug against A549, HeLa, Caco-2, and MCF-7 cell lines compared with normal fibroblast cells using MTT assay after 24 h of treatment was carried out.

Results showed a dose-dependent proliferation inhibition with IC_{50} values between 0.003 and 209.46 µg mL^{-1} for the tested compounds. On the other hand, the reference anti-proliferative drug cisplatin was less potent (0.13-3.99 µg mL^{-1}) than some of the tested compounds.

J. Braz. Chem. Soc. **2024**, *35*, 2, e-20230116

7 of 11

Compounds **9** and **10** showed potent cytotoxic activity against HeLa cancer cell lines in a concentration-dependent manner with IC_{50} of 0.85 µg mL^{-1} for compound **9** and 4.36 µg mL^{-1} for compound **10**, compared to 0.13 µg mL^{-1} for the control drug, cisplatin. On the other hand, compounds **9** and **10** had a potent effect on fibroblast control cells with an IC_{50} 4.49 and 5.22 µg mL^{-1}, respectively, but the IC_{50} was higher than cisplatin, 2.83 µg mL^{-1}. The least effect of all tested compounds was seen after treating the Caco-2 cell line.

Among the tested cancer cell lines, Hela cells showed a potent effect when treated with all tested compounds. The most potent effect was seen when Hela cell lines were treated with 0.003 µg mL^{-1} of compound **13**, compound **11** had the least effect. To determine if the selected compounds are more selective to tumor cells when compared to non-tumor ones, the selective action of a drug can be expressed by the selectivity index (SI). The selectivity index was calculated by comparing the cytotoxic activity (IC_{50} value) of each compound of each cancerous cell line against the fibroblast normal cell line. SI was calculated as a ratio of IC_{50} for a normal cell line (fibroblast IC_{50}) to IC_{50} value for the respective cancerous cell line using equation 1:[27]

$$SI = \frac{IC_{50} \text{ for fibroblast}}{IC_{50} \text{ for cancer cell}} \qquad (1)$$

The SI values higher than 1.0 describes a more selective anticancer agent. Compound **13** exhibited very high selectivity to the human cervical adenocarcinoma (HeLa) cell line (SI = 7332.1) and the highest one to the other cell lines. The highest the selectivity index the better the compound to be used as an anticancer candidate. All the tested compounds showed the highest index for HeLa cancer cells (SI ≥1.00) as indicated in Table 4.

The chemical structure of the tested compounds and the type of cancer cell seems to be directly related to their anti-proliferative activity. Likewise, all tested compounds showed the best antiproliferative activity on HeLa and human cervical adenocarcinoma cell lines, while Caco-2 cancer cell lines showed the least activity with the four tested compounds. Compound **13** was the best compound to show the highest anti-proliferative activity among the four tested cancer cell lines. When compared with cisplatin, the control drug, compound **13** showed much higher anti-proliferative activity on HeLa cancer cells. This makes it a highly potent compound against human cervical adenocarcinoma cancer.

Immunomodulatory properties of the selected compounds on TNF-α and IL-6 cytokines' release

Interleukin-6 (IL-6) and tumor necrosis factor α (TNF-α) are pleiotropic cytokines that play major roles

Table 3. IC_{50} of the synthesized compounds for the different cell lines used in the study and the control drug[a,b]

Cell	IC_{50} / (µg mL^{-1})				
	A549	HeLa	Caco-2	MCF-7	Fibroblast
Compound **9**	12.47 ± 0.70	0.85 ± 0.06	41.34 ± 4.72	10.30 ± 1.49	4.49 ± 0.73
Compound **10**	15.56 ± 1.93	4.36 ± 0.66	16.81 ± 0.36	11.42 ± 1.56	5.22 ± 0.52
Compound **11**	61.02 ± 4.84	13.78 ± 2.02	209.46 ± 28.78	61.44 ± 7.69	35.00 ± 5.38
Compound **13**	15.65 ± 0.54	0.003 ± 0.001	41.27 ± 2.85	17.58 ± 0.72	19.87 ± 1.40
Cisplatin	3.13 ± 0.53	0.13 ± 0.02	3.99 ± 0.67	1.51 ± 0.10	2.83 ± 0.12
DMSO (v/v) / %	0.33 ± 0.05	0.15 ± 0.02	23.40 ± 3.20	0.097 ± 0.02	0.13 ± 0.02

[a]Cells were cultured for 24 h in the presence of the indicated compounds; [b]data represent the mean of three independent experiments with three determinations in each, and were calculated using GraphPad Prism software (9.3.1)[21] by using nonlinear regression, dose response curve inhibition, log inhibitor *vs.* response equation. Values represent mean ± standard error of the mean (SEM). HeLa: human cervical adenocarcinoma, A549: adenocarcinoma human alveolar basal epithelial cells, MCF-7: human breast cancer, Caco-2: Caucasian colon adenocarcinoma, F2: human fibroblast cell lines; DMSO: dimethyl sulfoxide.

Table 4. Selectivity indexes (SI) represent IC_{50} for a normal cell line (fibroblast)/IC_{50} and for a cancerous cell line

	SI			
	Compound **9**	Compound **10**	Compound **11**	Compound **13**
A549	0.36	0.34	0.57	1.27
HeLa	5.28	1.20	2.54	7332.1
Caco-2	0.11	0.31	0.17	0.48
MCF-7	0.44	0.46	0.57	1.13

HeLa: human cervical adenocarcinoma; A549: adenocarcinoma human alveolar basal epithelial cells; MCF-7: human breast cancer; Caco-2: Caucasian colon adenocarcinoma.

8 of 11

J. Braz. Chem. Soc. **2024**, 35, 2, e-20230116

in cancer-associated cytokine networks. The levels of human IL-6 and TNF-α pro-inflammatory cytokines from the selected cancer cell lines were detected after being treated with the four selected synthesized compounds and compared with non-treated cells (control) and the control drug as indicated in Figures 3 and 4. The effect of DMSO was determined and did not show any significant effect on their release.

Compound **11** significantly increased the release of IL-6 cytokine in Caco-2, and MCF-7 cancer cell lines but not in HeLa cells or the normal fibroblast cells (Figure 3). Whereas it only increased the release of TNF-α in Caco-2, HeLa, and MCF-7 when cells were treated with 50 μg mL^{-1} of compound **11**. No effect was noticed on A459 cancer cells or the normal fibroblast cells (Figure 4). The effect of compound **13** on IL-6 release was relatively similar to compound **11** when HeLa and MCF-7 cancer cells were treated with all concentrations while no effect was noticed on Caco-2 and the normal fibroblast cells (Figure 3). On the other hand, only 50 μg mL^{-1} of compound **13** was able to stimulate Caco-2 cell lines to significantly release TNF-α while it had no effect on the other cells (Figure 4).

The effect of compounds **9** and **10** was relatively similar too. When Caco-2, HeLa, and fibroblast cells were treated with 25, and 50 μg mL^{-1} concentrations of compounds **9** and **10**, as a result, IL-6 was significantly released. On the other hand, when MCF-7 cancer cells were treated with all concentrations of compound **10** significantly increased the release of IL-6. Whereas only 50, 10, and 1 μg mL^{-1} concentrations of compound **9** were able to induce the release of IL-6 from MCF-7 cell lines (Figure 3). TNF-α release was also variable, only 50 μg mL^{-1} of compounds **9** and **10** were able to induce its release when MCF-7 cells and A459 cells were treated with them, respectively. Meanwhile, all used concentrations of compound **10** were able to induce the release of TNF-α cytokine on Caco-2 cell lines (Figure 4).

Compared with cisplatin, significant release of IL-6 and TNF-α was found for almost all cancer cells except Caco-2 cell lines which did not release TNF-α when treated with the four synthesized compounds. As indicated in Figures 3 and 4, the 50 μg mL^{-1} concentration of cisplatin was only able to induce the release of IL-6 for Caco-2 cell lines and TNF-α for A459, HeLa and MCF-7 cancer cell lines. None of the synthesized compounds or cisplatin was able to induce the release of TNF-α cytokines from the normal fibroblast cells (Figure 4). Meanwhile, fibroblast cells treated with 50 μg mL^{-1} of compound **10** and cisplatin induced IL-6 release while only 5 μg mL^{-1} of compound **9** significantly increased IL-6 release as indicated in Figure 3.

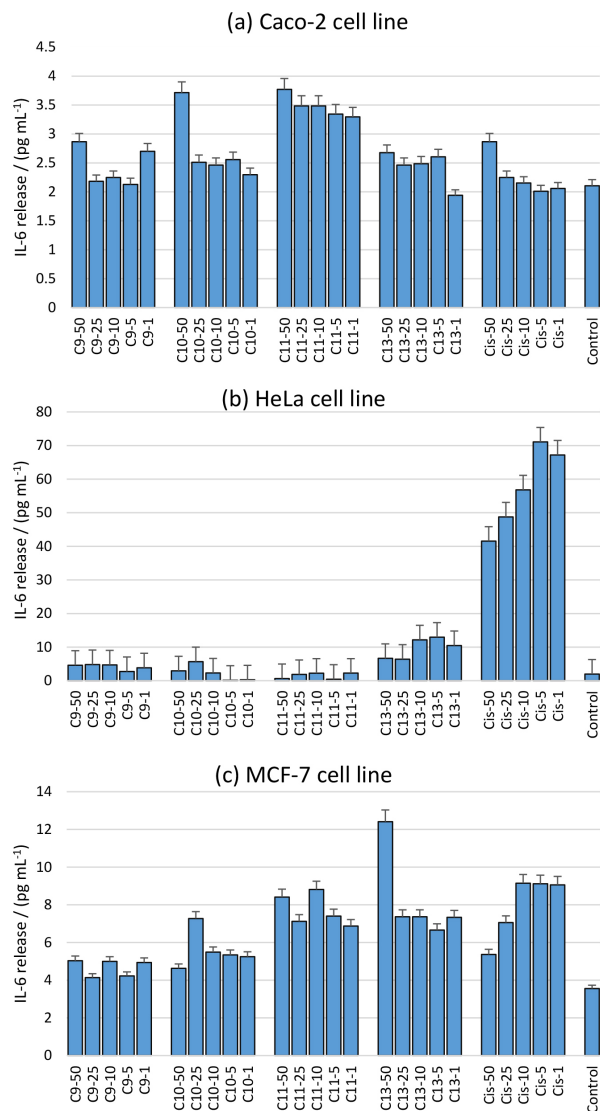**Figure 3.** The effect of different concentrations (50, 25, 10, 5, and 1 μg mL^{-1}) of the synthesized compounds **9**, **10**, **11** and **13** on the release of IL-6 pro-inflammatory cytokine on cancer cell (a) Caco-2, (b) HeLa and (c) MCF-7 cell lines. Data represent the mean concentration pg mL^{-1} of triplicates ± standard error of the mean (SEM). Differences were considered significant at *P* < 0.01 *vs*. control.

The inflammatory process was found to significantly play a role in tumorigenesis with increasing evidence that pro-inflammatory cytokines like interleukin-6 and tumor necrosis factor-α are involved in the development of cancer. They have shown a potential role in colorectal cancer (CRC) pathogenesis as they were found to be elevated in CRC patients.[28-30] They were also found to be associated with the progress and prognosis of metastatic breast cancer, lung cancer, and other various cancer types.[31-33] This gives a promising effect on clinical trials. The effect of the selected compounds was mostly cancer specific, their influence on the normal fibroblast cells did not enhance the release of TNF-α pro-inflammatory cytokine
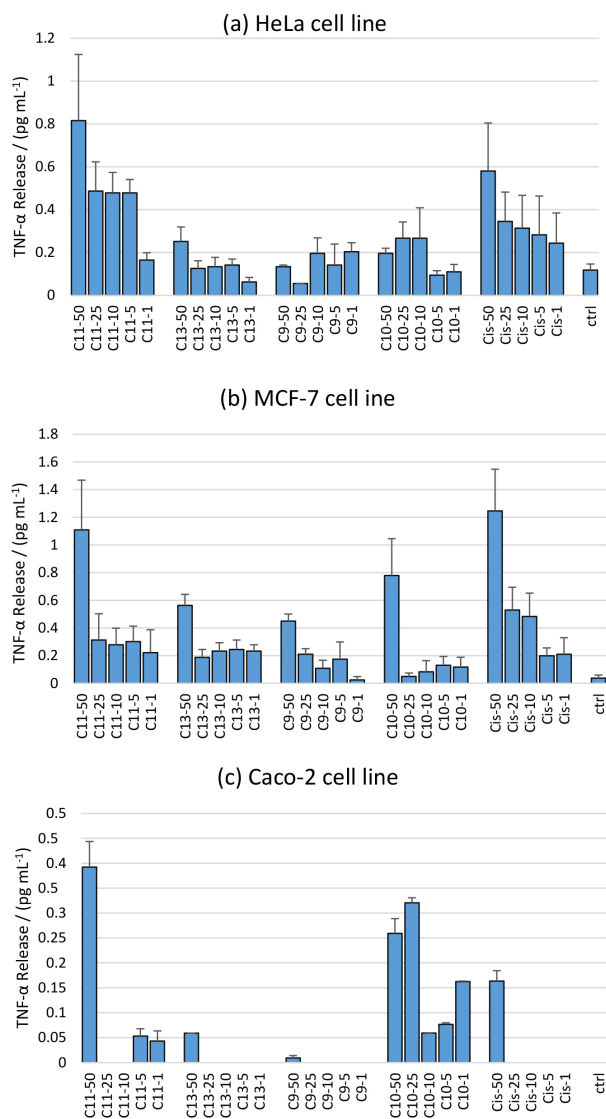
Figure 4. The effect of different concentrations (50, 25, 10, 5, and 1 µg mL^{-1}) of synthesized compounds **9**, **10**, **11** and **13** on the release of TNF-α pro-inflammatory cytokine on cancer cell lines (a) HeLa, (b) MCF-7 and (c) Caco-2 cell lines. Data represent the mean concentration pg mL^{-1} of triplicates ± SEM. Differences were considered significant at *P* < 0.01 *vs.* control.

while IL-6 was only enhanced at either 5 or 50 µg mL^{-1} of compounds **9** and **10**, respectively, but not with any other tested concentration. Targeting IL-6 and TNF-α is a promising anticancer therapy, yet their effect still needs to be explored by more future studies. A strong association was revealed between inflammation and cancer showing high IL-6 levels in the tumor microenvironment.[34-36] For that, blocking IL-6 cytokine could be a potential therapeutic strategy for the treatment of many cancers. Most of our synthetic compounds induced IL-6 production in most of the cancer cell lines, but they exerted cancer-specific effects.

Compound **11** blocked IL-6 release on HeLa cancer cells with all used concentrations while compound **13**

stimulated IL-6 release in all types of tested cancer cells. Regarding compounds **9** and **10** concentrations did block IL-6 release in almost all cell lines except for compound **10** which was able to stimulate IL-6 release in A459 and MCF-7 cancer cell lines with all used concentrations. This makes compound **11** the best among them but only for HeLa cancer cells.

Although TNF-α cytokine is considered a potent inflammatory cytokine inducing complex immune responses, it has a complicating paradoxical role in cancer. On the one hand, it has an anticancer effect by inducing cancer cell death that can be used for cancer therapy. On the other hand, it stimulates survival, migration, proliferation, and angiogenesis in most cancer cells that are resistant to TNF-induced cytotoxicity leading to tumor promotion. Accordingly, TNF is a double-edged sword that is either pro- or anti-tumorigenic.[37] In this concern, our compounds showed variable effects on TNF-α cytokine depending on the cancer cell line used. Almost all tested synthetic compounds were able, at least in one low concentration, to block the release of TNF-α in one cancer cell type while 50 µg mL^{-1} amount were able to increase its levels in some cancer cells. On the other hand, compound **10** induced TNF-α release with all tested concentrations. In this regard and depending on the cancer cell type and what is requested for its treatment, one of the selected compounds can be employed as a potential therapy.

Conclusions

In conclusion, some benzoxazepine derivatives are successfully prepared and two of these derivatives produced X-ray structures. The benzoxazepine derivatives could be potent chemotherapeutic candidates according to the results obtained after anti-microbial, anti-cancer and anti-inflammatory assays. There is an expected anti-cancer and anti-inflammatory potential for the studied synthesized compounds depending on the cancer cell type. The benzoxazepine derivatives displayed cytotoxicity against selected solid tumor cell lines with varying effects on the release of human interleukin-6 (IL-6) and tumor necrosis factor-α (TNF-α).

Supplementary Information

Crystallographic data (excluding structure factors) for the structures in this work were deposited in the Cambridge Crystallographic Data Centre as supplementary publication number CCDC 2233684 and 2233684 for compounds **13** and **10**, respectively. Copies of the data can be obtained, free of charge, via https://www.ccdc.cam.ac.uk/structures/.

10 of 11

J. Braz. Chem. Soc. **2024**, *35*, 2, e-20230116

Supplementary information (¹H NMR, ¹³C NMR, DEPT spectra and HRMS for compounds **2**, **3**, **8**, **9**, **10**, **11** and **13**) is available free of charge at http://jbcs.sbq.org.br as PDF file.

Acknowledgments

References

1. Liao, Y.; Venhuis, B. J.; Rodenhuis, N.; Timmerman, W.; Wikström, H.; Meier, E.; Bartoszyk, G. D.; Böttcher, H.; Seyfried, C. A.; Sundell, S.; *J. Med. Chem.* **1999**, *42*, 22235. [Crossref]

2. Bajaj, K.; Srivastava, V. K.; Lata, S.; Chandra, R.; Kumar, A.; *Indian J. Chem.* **2003**, *34*, 1723. [Crossref]

3. Bajaj, K.; Srivastava, V. K.; Kumar, A.; *Indian J. Chem.* **2003**, *34*, 1149. [Crossref]

4. Goodnow, R. A.; Galley, G.; Peters, J.; *WO pat. 2004100958 A1* **2004**.

5. Sung, H.; Ferlay, J.; Siegel, R. L.; Laversanne, M.; Soerjomataram, I.; Jemal, A.; Bray, F.; *CA Cancer J. Clin.* **2021**, *71*, 209. [Crossref]

6. Greten, F. R; Grivennikov, S. I.; *Immunity* **2019**, *51*, 27. [Crossref]

7. Tang, J.; Jiang, Y.-L.; Wang, B.-X.; Shen, Y.-M.; *Z. Naturforsch.* **2014**, *7-8*, 283. [Crossref]

8. Pecher, J.; Waefelaer, A.; Poultier, P.; *Bull. Soc. Chim. Belg.* **1977**, *86*, 1003. [Crossref]

9. Pecher, J.; Waefelaer, A.; *Bull. Soc. Chim. Belg.* **1978**, *87*, 911. [Crossref]

10. El Gihani, M. T.; Heaney, H.; Shuhaibar, K. F.; *Synlett* **1996**, *9*, 871. [Crossref]

11. Srinivasulu, V.; Shehadeh, I.; Khanfar, M. A.; Malik, O. G.; Tarazi, H.; Abu-Yousef, I. A.; Sebastian, A.; Baniowda, N.; O'Connor, J.; Al-Tel, T. H.; *J. Org. Chem.* **2019**, *84*, 934. [Crossref]

12. Garg, N.; Chandra, T.; Archana; Jain, A. B.; Kumar, A.; *Eur. J. Med. Chem.* **2010**, *45*, 1529. [Crossref]

13. Grunewald, G. L.; Dahanukar, V. H.; Ching, P.; Crisclone, K. R.; *J. Med. Chem.* **1996**, *39*, 3539. [Crossref]

14. Walker, G. N.; Smith, R. T.; *J. Org. Chem.* **1971**, *36*, 305. [Crossref]

15. Derieg, M. E.; Sternbach, L. H.; *J. Heterocycl. Chem.* **1966**, *3*, 237. [Crossref]

16. CIBA Ltd.; *Fr. Pat. 1 463 402*, **1966**.

17. Levan, K. R.; Root, C. A.; *Inorg. Chem.* **1981**, *20*, 3566 [Crossref]; Levan, K. R.; Root, C. A.; *J. Org. Chem.* **1981**, *46*, 2404. [Crossref]

18. Mizyed, S.; Ashram, M.; Awwadi, F. F.; *Arkivoc* **2011**, *10*, 277. [Crossref]

19. Ashram, M.; Awwadi, F. F.; *Arkivoc* **2019**, 142. [Crossref]

20. Ashram, M.; *J. Chem. Soc., Perkin Trans. 2* **2002**, *10*, 1662 [Crossref]; Mizyed, S.; Marji, D.; Kiwan, R.; *Jordan J. Chem.* **2013**, *8*, 71. [Crossref]

21. Motulsky, H. J.; Christopoulos, A.; *GraphPad*; San Diego, CA, USA, 2003. [Link] accessed in July 2023

22. *CrysAlisPro*, version 1.171.41.112a, Rigaku Corporation, Oxford, UK.

23. Dolomanov, O.V.; Bourhis, L. J.; Gildea, R. J.; Howard, J. A. K.; Puschmann, H.; *J. Appl. Cryst.* **2009**, *42*, 339. [Crossref]

24. Sheldrick, G. M.; *Acta Cryst.* **2015**, *A71*, 3. [Crossref]

25. Sheldrick, G. M.; *Acta Cryst.* **2015**, *C71*, 3. [Crossref]

26. Fujioka, H.; Murai, K.; Ohba, Y.; Hiramatsu, A.; Kita, Y.; *Tetrahedron Lett.* **2005**, *46*, 2197. [Crossref]

27. Bartmańska, A.; Tronina, T.; Popłoński, J.; Milczarek, M.; Filip-Psurska, B.; Wietrzyk, J.; *Molecules* **2018**, *23*, 2922. [Crossref]

28. Cruz-López, O.; Ner, M.; Nerín-Fonz, F.; Jiménez-Martínez, Y.; Araripe, D.; Marchal, J. A.; Boulaiz, H.; Gutiérrez-de-Terán, H.; Campos, J. M.; García, A. G.; *J. Enzyme Inhib. Med. Chem.* **2021**, *36*, 1551. [Crossref]

29. Chung, S. S.; Wu, Y.; Okobi, Q; Adekoya, D.; Atefi, M.; Clarke, O.; Dutta, P.; Vadgama, J. V.; *Mediators Inflamm.* **2017**, ID 5958429. [Crossref]

30. Borowczak, J; Szczerbowski, K; Maniewski, M; Kowalewski, A.; Janiczek-Polewska, M.; Szylberg, A.; Marszałek, A.; Szylberg, Ł.; *Biomedicines* **2022**, *10*, 1670. [Crossref]

31. Ueda, T.; Shimada, E.; Urakawa, T. J.; *J. Gastroenterol.* **1994**, *29*, 23. [Crossref]

32. Tripsianis, G.; Papadopoulou, E.; Anagnostopoulos, K.; Botaitis, S.; Katotomichelakis, M.; Romanidis, K.; Kontomanolis, E.; Tentes, I.; Kortsaris, A.; *Neoplasma* **2014**, *61*, 205. [Crossref]

33. Kim, M. S.; Han, J. Y.; Kim, S. H.; Kim, H. Y.; Jeon, D.; Lee, K.; *J. Toxicol. Sci.* **2018**, *43*, 485. [Crossref]

34. Liu, X.; Meng, L.; Chen, L.; Liang, Y.; Wang, B.; Shao, Q.; Wang, H.; Yang, X.; *J. Cell. Mol. Med.* **2020**, *24*, 2284. [Crossref]

35. Kumari, N; Dwarakanath, B. S.; Das, A.; Bhatt, A. N.; *Tumor Biol.* **2016**, *37*, 11553. [Crossref]

36. Rossi, J. F.; Lu, Z. Y.; Jourdan, M.; Klein, B.; *Clin. Cancer Res.* **2015**, *15*, 1248. [Crossref]

37. Shen, J.; Xiao, Z.; Zhao, Q.; Li, M.; Wu, X.; Zhang, L.; Hu, W.; Cho, C. H.; *Cell Prolif.* **2018**, *51*, e-12441. [Crossref]